
A further study of control for a pendulum-driven cart

Hongnian Yu*

Faculty of Computing, Engineering and Technology,
Staffordshire University,
Stafford, ST18 0AD, UK
E-mail: h.yu@staffs.ac.uk
*Corresponding author

Taicheng Yang

School of Engineering and Information Technology,
Sussex University,
Brighton, BN1 9QT, UK
E-mail: taiyang@sussex.ac.uk

Yang Liu and Sam Wane

Faculty of Computing, Engineering and Technology,
Staffordshire University,
Stafford, ST18 0AD, UK
E-mail: y.liu@staffs.ac.uk
E-mail: s.o.wane@staffs.ac.uk

Abstract: Recently, the control of a ‘pendulum-driven cart’ has attracted some considerable research interest. One of the reasons is that the mechanism studied is very similar to that of an ‘actively-driven capsule robot’ which is still under development and will have wide potential medical applications. In this paper, we study the pendulum-driven cart system from a control viewpoint, and use it as a benchmark to explore a new robust control approach which achieves better performance than those presented in a previous paper. The controller designed is also robust against uncertainties in plant parameters and very simple to implement. The extensive simulation studies and experimental results have demonstrated the proposed control approach.

Keywords: pendulum-driven; robust control; inverted pendulum; underactuated system; propulsive mechanism.

Reference to this paper should be made as follows: Yu, H., Yang, T., Liu, Y. and Wane, S. (2008) ‘A further study of control for a pendulum-driven cart’, *Int. J. Advanced Mechatronic Systems*, Vol. 1, No. 1, pp.44–52.

Biographical notes: Hongnian Yu is currently a Professor of Computer Science and Head of the MCDS Research Group at Staffordshire University. He has extensive research experience in modelling and control of robots and mechatronics devices and neural networks, mobile computing, modelling, scheduling, planning and simulations of large discrete event dynamic systems, RFID with applications to manufacturing systems, supply chains, transportation networks and computer networks. He has published over 140 research papers and held several grants from EPSRC, the Royal Society, and other funding bodies. He is a member of the EPSRC Peer Review College and serves on various conferences and academic societies.

Taicheng Yang received his MSc and PhD both in Control Engineering in 1981 from Shanghai Tong-Ji University, China, and in 1987 from the University of Manchester Institute of Science and Technology, U.K., respectively. He joined the School of Engineering and Information Technology, University of Sussex, U.K., as a Lecturer in 1990. He was promoted to a Reader in the School in 1999. His current research interests include networked control systems, wind power and power system control and control applications.

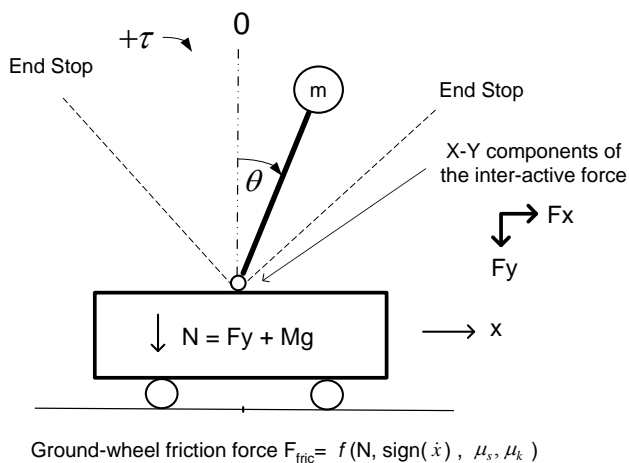
Yang Liu received his BEng in Automation from Hunan University, China, in 2003 and MSc in Control Systems from University of Sheffield, UK, in 2005. He is currently a PhD student with the Faculty of Computing, Engineering, and Technology, Staffordshire University, UK. His research interests include control of underactuated mechatronic systems, robotics for medical applications and control of a capsule robot for medical endoscope.

Sam Wane obtained his Masters in Electronic Engineering from the University of Hull in 1996. He went on to develop software for the 'Handy-1', a rehabilitation robot to aid people with no arms to feed themselves. His improvements to the robot allowed it to shave, wash, brush teeth and play games. He then spent two years designing and developing biscuit packing robots for the food industry. Since 2000, he has been working as a Senior Lecturer in robotics and control at Staffordshire University and pursuing a part-time PhD where he is developing a wirelessly controlled robot propulsion mechanism as part of the MCDS team.

1 Introduction

The problem of the 'pendulum-driven cart' was first proposed in Li et al. (2005), see Figure 1. The pendulum-driven cart is a two-degrees-of-freedom underactuated system with one actuator only. A motor is attached to the pivot of the pendulum as the actuator. The purpose of studying this system is to control the cart locomotion by swinging the pendulum. Recently, the research on the proposed system has attracted growing attention. A four-step motion and dynamic modelling of the pendulum-driven cart-pole system is proposed in Li et al. (2005). An open-loop control law with six-step motion strategy is studied in Liu et al. (2007). Optimisation and closed-loop control of the pendulum-driven cart-pole system are investigated in Yu et al. (2008). An initial experimental study using the open-loop control strategy is conducted in Wane et al. (2007). The purpose of this paper is to study the pendulum-driven cart system from a control point of view, and we will use it as a benchmark to explore a new robust control approach.

Figure 1 Pendulum-driven cart



This paper investigates control strategies of a pendulum-driven cart-pole system. The pendulum-driven cart-pole system is a reversed experiment from the classical inverted pendulum cart system. We put torque on the pendulum pivot, instead of the force on the cart. The purpose of this research is to make the cart track a designed trajectory by using a control torque. The difference between the classical inverted pendulum cart system and the pendulum-driven cart-pole system is that the former is a stabilisation problem and the latter is a tracking problem. A similar idea is proposed in Chernousko (2001), which is to control a

two-link mechanism along a horizontal plane by using the torque on the hinge joint. A two-mass system with optimum rectilinear motion is proposed in Chernousko (2002). Generally, these propulsion mechanisms have similar properties which are controlled by internal force and static friction. The key control issue is to control the propulsion part properly to drive the entire body to a desired position.

With an inverted pendulum on a cart, instead of moving the cart to balance the pendulum, a torque motor is mounted on the cart to drive the pendulum to swing. The output of the torque motor, τ , is the control law to be designed. The system has two degrees of freedom in movement: the rotational movement of the pendulum and the translational movement of the cart. The interactions between them are through a force at the pivot point shown in Figure 1. The dynamic equations for this system are (Liu et al., 2007; Yu et al., 2008):

$$\begin{aligned} F_x &= m\ddot{x} - ml\ddot{\theta}\cos\theta + ml\dot{\theta}^2\sin\theta \\ F_y &= mg - ml\ddot{\theta}\sin\theta - ml\dot{\theta}^2\cos\theta \\ ml^2\ddot{\theta} &= \tau + mgl\sin\theta + ml\dot{x}\cos\theta \\ M\ddot{x} &= F_{xc} - F_{fric}(F_y + Mg, \text{sign}(\dot{x}), \mu_s, \mu_k) \\ F_{xc} &= -F_x \end{aligned} \quad (1)$$

where $\text{sign}(\dot{x}) = 0, 1, -1$ when $\dot{x} = 0, > 0, < 0$, respectively. This model is simulated by using simulink with the nominal data below:

- m : mass of the ball = 0.05 kg
- M : mass of the cart = 0.5 kg
- l : the length of the rod = 0.3m (the mass = 0)
- μ_s : coefficient of static friction = 0.02
- μ_k : coefficient of kinetic friction = 0.5 μ_s

If the pendulum moves anticlockwise quickly, the cart will move forward (x increases), and vice versa. The purpose of the control is to make a big net x increase in a completed pendulum swing cycle, and in particular to have a big net x increase in a given period of time. This can be measured by the cart's average speed: the net x increase over a period of time divided by the time taken. To achieve this, apart from a quick anticlockwise movement of the pendulum, the clockwise swing of the pendulum must be slower so that the induced force to move the cart backwards is smaller. In addition, to achieve a high average cart speed the time taken for a complete swing cycle should be small.

In Li et al. (2005), a dynamic model of the 'pendulum-driven cart' is presented, and an open-loop control of the

four-step pendulum motion generation is derived. Although there is no simulation result presented in Li et al. (2005), a working LEGO toy setup is reported to demonstrate the idea. In Yu et al. (2008), a more systematic modelling and motion analysis approach is presented. Based on this and a newly proposed six-step control, two control methods and some simulation results are presented. Method 1 gives an average speed of 0.37 cm/s.; and Method 2 achieves a much better result of 1.31 cm/s. In addition, a partial feedback linearisation scheme for closed-loop control is proposed. In parallel with this, a more sophisticated experimental setup is being constructed (Wane et al., 2007). In this paper, we first present a completely different non-linear control method, Method 3, which achieves an average speed of 1.87 cm/s, 43% more than that achieved by Method 2 in Yu et al. (2008). The closed-loop control system also has excellent robust stability as demonstrated by the results presented in the next section, Section 2. A further exploration of the significance of research on the system is presented in Section 3. Experimental results are given in Section 4. A brief conclusion is summarised in Section 5.

2 A new control method – simple switch control

Instead of the mathematical-oriented approaches used in Li et al. (2005), Liu et al. (2007) and Yu et al. (2008) which rely on many equations derived from the original equations, our new control method is mainly based on some key concepts in advanced non-linear control and some valuable physical insights. On the other hand, our new method does present a challenging theoretical problem: for the non-linear feedback control designed in this paper to prove the existence of a locally stable limit cycle.

The basic model and the parameter values used for the controller design in this paper are the same as those in Yu et al. (2008). Some improvement in the modelling in this paper is to reflect some practical considerations:

- 1 The angle movement of the pendulum is limited by the two end stops. When the pendulum angle $|\theta| > \theta_{\max}$ (θ_{\max} is set to one radian, 57.3 degrees in a simulation, the simulation will stop and the system is considered unstable.
- 2 As a design constraint, the maximum control torque τ_{\max} is set to 0.45 Nm in Yu et al. (2008), the actual maximum control signals are 0.4 Nm and 0.5 Nm for Method 1 and Method 2, respectively.
- 3 We distinguish between the coefficient of kinetic friction μ_k ($\mu_k = 0.01$ in Yu et al. (2008) and also here) and the coefficient of static friction μ_s . μ_s is introduced in this paper and we assume that $\mu_s = 2\mu_k$.

This is in line with other literatures where both coefficients of kinetic friction and static friction are considered.

Figure 2 Angle time responses under Method 3 (see online version for colours)

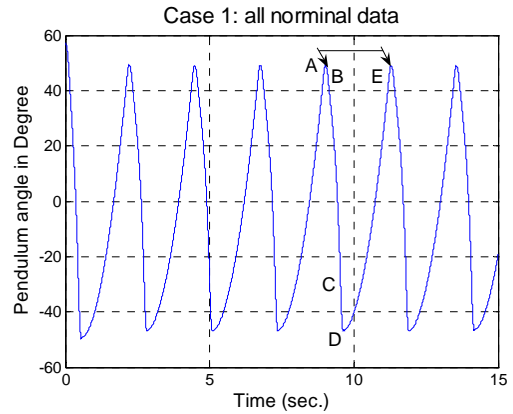


Figure 3 Cart position responses under Method 3 (see online version for colours)

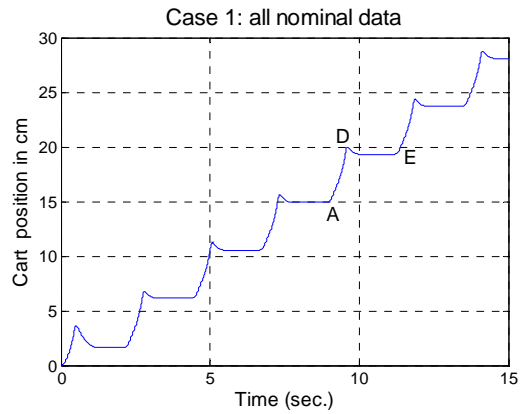
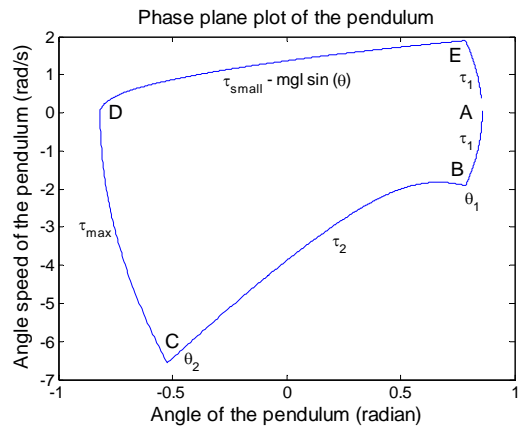


Figure 4 Phase plane plot of angle position-speed (see online version for colours)



Figures 2 and 3 are plots of the time responses of the pendulum angle and the cart position when the control of Method 3 is applied. (The new control method is described in the following paragraphs). Initially, the pendulum rests on the right-hand end stop, $\theta_0 = \theta_{\max}$ and $\dot{\theta}_0 = 0$; and the cart is at a standstill $x_0 = 0$ and $\dot{x}_0 = 0$. After the control is applied, the system soon settles to a regular swing/moving

pattern shown in Figures 2 and 3. At $t = 15$ sec the cart has made a net movement of 28.1 cm, giving an average speed of 1.87 cm/s. The response in Figure 3 is similar in shape to that presented in Yu et al. (2008), but shows a fast net forward movement. Figure 4 is a phase-plane plot of $\theta - \dot{\theta}$. The controls applied, τ_1, τ_2, \dots , are also shown in the figure. This figure is for one of the repeated swing cycles: $9.02 < t < 11.28$, indicated as a sequence of A–B–C–D–E–A (also shown in Figure 2). In addition to Figure 3, the cart movement during the cycle is given in Figure 5 as a plot of x against θ .

At the starting point of the cycle, ‘A’, when the pendulum is in its right-most position $\theta = \theta_{right}$, a control torque $\tau_1 = -k_1 \tau_{max}$ ($k_1 = 0.5$) is applied. This relatively high torque not only moves the pendulum anticlockwise, but also triggers the cart’s movement in the $x+$ direction, also see Figure 2. When $\theta = \theta_1$ ($\theta_1 = 45^\circ$, 0.79 radian) at point ‘B’ in Figure 4, a smaller torque $\tau_2 = -k_2 \tau_{max}$ ($k_2 = 0.2$) is applied. This torque makes the pendulum continue its movement at an accelerated pace, and the induced inter-active force F_x drives the cart to continue its movement in the $x+$ direction. When $\theta = \theta_2$ ($\theta_2 = -30^\circ$, -0.52 radian), at point ‘C’ in Figure 4, a break torque $\tau = \tau_{max}$ is applied. The pendulum decelerates but continues to move in an anticlockwise direction until at its left-most position $\theta = \theta_{left}$, i.e., point ‘D’ in Figure 4. At this point, the pendulum changes its direction of movement. Once this is detected, a new torque $\tau_3 = \tau_{small} - mg \sin(\theta)$, ($\tau_{small} = 0.005 Nm$) is applied. The $mg \sin(\theta)$ term in the control is to cancel the ball’s gravity torque so that the pendulum moves clockwise in a constantly-accelerating manner. When the pendulum moves slowly to point ‘E’, $\theta = \theta_1$, a new control $\tau = \tau_1$ applies again. The four-stage piece-wise feedback control u of Method 3 can be summarised in Table 1.

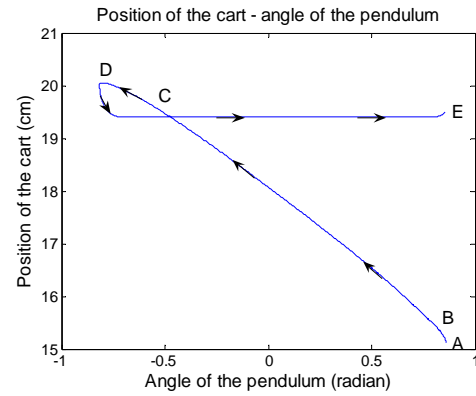
Table 1 Controls of Method 3

Stage	Condition(s)	U	Locus
1	$\theta > \theta_1$	τ_1	E–A–B
2	$\theta_1 \geq \theta \geq \theta_2$ and $\dot{\theta} < 0$	τ_2	B–C
3	$\theta < \theta_2$ and $\dot{\theta} < 0$	τ_{max}	C–D
4	$\dot{\theta} \geq 0$ and $\theta \leq \theta_1$	τ_3	D–E

The mathematical representation of the control law (Method 3) in Table 1 is

$$\tau = \begin{cases} \tau_1 & \theta > \theta_1 \\ \tau_2 & \theta_1 \geq \theta \geq \theta_2 \text{ and } \dot{\theta} < 0 \\ \tau_{max} & \theta < \theta_2 \text{ and } \dot{\theta} < 0 \\ \tau_3 & \theta \leq \theta_1 \text{ and } \dot{\theta} \geq 0 \end{cases} \quad (2)$$

Figure 5 Position – angle plot of Case 1 (see online version for colours)



It is shown in Figure 5 that the cart’s forward movement is mainly in control stage 2, from point B to point C. When the pendulum changes its swing direction around point D, the induced force causes the cart to move backwards slightly. After that, due to the low-speed clockwise movement of the pendulum, the induced force is not big enough to overcome the friction force and the cart remains at a standstill. It is worthwhile pointing out that

- 1 The friction force is the key for the system to work. If no friction $\mu_s = \mu_k = 0$, then from a physical point of view and from the simulation (Figure 7), one can see that the cart cannot make net forward movement – the cart makes the same amount of forward and backwards movement, though at different speeds.
- 2 When the cart is moving, the friction force – its magnitude depends on the normal force N applied to the contact surface and is independent of the cart speed – is different from a damping force.

An inverted pendulum is inherently unstable and the system is under-actuated. Before any performance consideration, the stability/robust stability must first be guaranteed. For this system, the stability condition for the pendulum angle movement is not ‘stability around an equilibrium point’, but ‘bounded’ or ‘a stable limit cycle’ and can be considered as $\forall t > 0, |\theta| \leq \theta_{max}$. This can also be directly shown in Figure 4 as the ± 1 radian boundaries. In addition, $\theta_{max} - \theta_{right}$ at point A and $\theta_{max} + \theta_{left}$ at point D is the right and left stability margin, respectively. The loci in Figure 4 are actually a locally stable limit cycle and one can indeed prove it. This is our planned further work and will be presented in a full-length journal paper. Here, as an example to explain the robust stability, the point corresponding to the initial condition at $t = 0$, $\theta_0 = \theta_{max}$ and $\dot{\theta}_0 = 0$ is outside the limit cycle initially. Under the control of Method 3, the system response is settled to the phase-plane limit cycle as shown in Figures 2 and 4. Therefore, one can see that the system is robust against disturbances – a disturbance will initially divert the system response away from the limit-cycle, then under the designed control, the system response will settle to stable oscillations after some transients as shown in Figure 2.

Where uncertainties in the plant parameters are considered, proofs of robust stability are much harder to find. However, Method 3 is a form of sliding mode control which is inherently robust. The parameter uncertainties concerned in this system are friction coefficients: the mass of the ball and the mass of the cart. Table 2 summarises the results of some simulation tests. A nominal value of $m = 0.05$ for control stage 4: $\tau_3 = \tau_{small} - mg \sin(\theta)$ is used for all simulations. In Table 2, the first column is the case number; the second column shows the change of the plant parameter(s) in percentage; and the last column is the value of $x(t = 15)$ in centimetres at the end of the simulations. In all cases studied, the simulation plots show a stable limit cycle response. In most cases, except 9 and 11, the cart position plots have a very similar shape to that shown in Figure 3. For example, Figure 6 shows the simulation result of Case 13: the cart position when the mass of the ball is reduced by 40% (note: although in a similar shape, the y-axis scale in Figure 6 is only half of that in Figure 3). More simulation plots are not presented here but can be found in Yu et al. (2008).

Table 2 Cart positions at $t = 15$ sec

Case	Parameter change	$x(t = 15)$
1	Nominal parameters	28.1
2	$\mu_s, \mu_k +25\%$	21.2
3	$\mu_s, \mu_k +50\%$	14.8
4	$\mu_s, \mu_k +75\%$	8.31
5	$\mu_s, \mu_k +100\%$	2.00
6	$\mu_s, \mu_k -25\%$	35.7
7	$\mu_s, \mu_k -50\%$	40.9
8	$\mu_s, \mu_k -75\%$	43.7
9	$\mu_s, \mu_k -100\% = 0$	N/A
10	$m +20\%$	32.5
11	$m +40\%$	10.4
12	$m -20\%$	21.3
13	$m -40\%$	13.7
14	$M +20\%$	19.0
15	$M +40\%$	12.7
16	$M -20\%$	42.5
17	$M -40\%$	68.2

Figure 7 shows that if there is no wheel-ground friction $\mu_s = \mu_k = 0$, the cart will not make net movement in the $x+$ direction (Case 9). Figure 8 shows that if the mass of the ball is increased by 40%, the cart initially has a big backwards movement and after $t > 10$ sec, it settles to a regular pattern of movement (Case 11).

The implementation of the control given in Table 1 is extremely simple. If necessary, Stage 3 control law $\tau_3 = \tau_{small} - mgl \sin(\theta)$ can be pre-calculated and stored as

a look-up table for online use. The inputs required for the controls are θ and $\text{sign}(\dot{\theta})$. θ can be obtained from an encoder and $\text{sign}(\dot{\theta})$ can be known from successive readings of θ from the encoder. Therefore, only the measurement of θ is required for the designed control.

Figure 6 Cart position responses for Case 13 (see online version for colours)

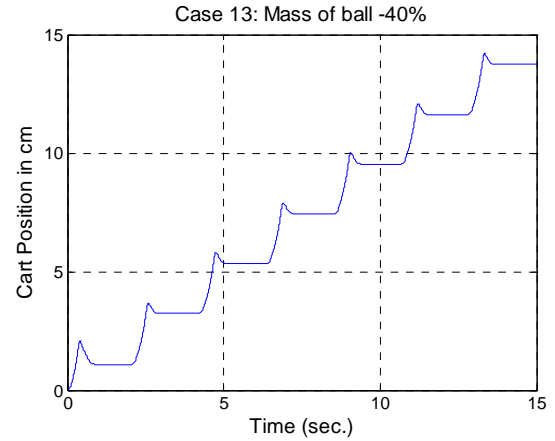


Figure 7 Cart position responses for Case 9 (see online version for colours)

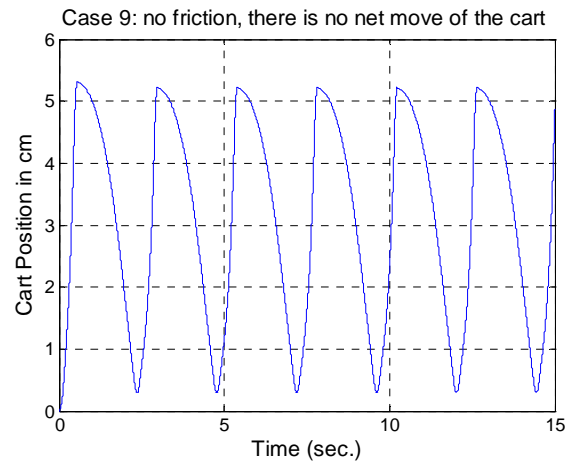


Figure 8 Cart position responses for Case 11 (see online version for colours)

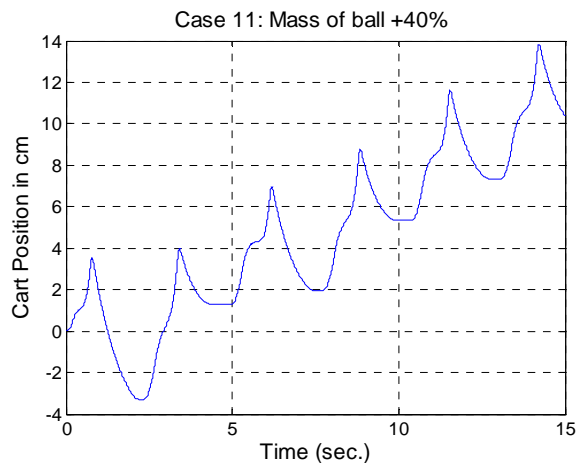
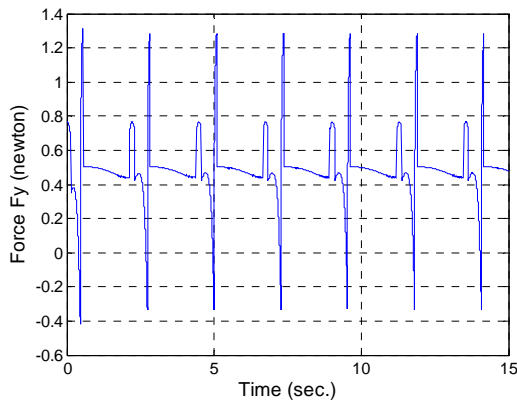


Figure 9 Induced force F_y (Case 1) (see online version for colours)



One physical constraint of the system is that the cart must always be in contact with the ground surface, i.e., $N > 0 \forall t > 0$. In our simulation model, this condition is tested in every simulation step. If this is violated, the simulation will stop and an error message will be given. Figure 9 is a plot of F_y for Case 1. Since $Mg = 4.9$, $N = F_y + Mg > 0 \forall t > 0$.

There are five design parameters $\theta_1, \theta_2, k_1, k_2$ and τ_{small} in Method 3. At first one may think that some numerical optimisation methods (apparently there is no analytical solution) can be applied to obtain a set of five parameters to maximise the net x movement in a given period of time. However, such an optimisation may affect the robustness. For example, for the nominal plant parameters, one may increase τ_{small} to a bigger value so that the induced force is still not big enough to make the cart to move in the negative direction. This τ_{small} then will reduce the time taken for the movement corresponding to locus D–E in Figure 4 and therefore increase the overall average speed. However, if the mass of the cart is reduced from its nominal value, Mg , N and the friction force will reduce which may actually cause the cart to move backwards and reduce the average speed in the $x+$ direction. Therefore, one needs to find the right balance between performance and robustness.

In our control method, the selection of the values for $\theta_1, \theta_2, k_1, k_2$ and τ_{small} is mainly based on physical insights and is assisted by organised simulation studies. For example, when the value of θ_2 (point C in Figure 4) is considered, if one moves ‘C’ towards the left then there will be more cart movement in the $x+$ direction. However, on the other hand, one needs to consider that after θ_2 the maximum available torque is applied to break the pendulum’s anticlockwise movement to prevent it hitting the left-end end stop. There should preferably be a suitable left-side stability margin $\theta_{max} + \theta_{left}$ at point D for robustness. From this point of view, there is a ‘left limit’ for the value of θ_2 which also depends on the speed of the pendulum at point C.

3 Discussion

From the two previous papers (Li et al., 2005 and Yu et al., 2008), one can see that controller design can be very complicated involving a great deal of mathematical manipulations even for this low-order system. The non-linear dynamics involved, in particular the key role of friction, is not simple by any means. Therefore, from the control system point of view, different design methods can be developed for this system for comparison. More significantly, this system may be used as a benchmark to explore a new concept of ‘optimal control’ as discussed below.

The widely used quadratic cost function in optimal control has some major limitations in many applications

- 1 ‘sensor cost’ is not reflected in the cost function
- 2 while the $u^2(t)$ term in the cost function is linked with the control energy which contributes to the running cost, $\max(|u(t)|)$ is not included.

However, $\max(|u(t)|)$ is directly linked with the capital cost of the actuator and its size, and these are important factors to be included in many practical designs. To overcome these limitations, we propose to use this ‘pendulum-driven cart problem’ to design a controller to maximise a new performance index: for a set of three different coefficients of friction, the average distance travelled by the cart in 15 seconds. The weighted ‘sensor cost’ is deducted from the index – it penalises a method if more measurements (sensors) are required for the control. The weighted ‘actuator cost’ is also deducted from the index – it penalises a high $\max(|u(t)|)$ required for the control.

Apart from the above, it is interesting to compare this system with the benchmark system previously studied by control professionals, i.e., the well-known ‘inverted pendulum on a cart’ where the cart is driven by an actuator. This is a stabilising controller design problem and ‘linearisation around an equilibrium point’ is often used for controller design. In the problem of the ‘pendulum-driven cart’ here, the non-linear model has to be used for the design.

In many applications it can also be seen, and the system studied in this paper is used as an example, that ‘controller design cannot be simply formulated as a multi-objective-constrained optimisation problem’. This is certainly research needing to be pursued beyond general academic study. Even in ‘small-scale’ systems, designers have to make a balanced choice to meet a number of specifications and with the lowest possible cost. Apparently, there is no ‘pure’ analytical solution to this challenge. Therefore we applied a different approach: ‘method based on important concepts and physical insights assisted by organised simulation studies’. This approach appears to have worked very well for the system studied here. Since the mechanism studied is very similar to that of an ‘actively-driven capsule robot’ which has wide medical applications, further study on this system would bring significant benefits to robotic and control professionals.

4 Experimental set-up and results

In this section, the experimental setup of the pendulum-driven cart-pole system and the experimental results are shown. The objective of this experiment is to demonstrate the proposed ideas.

The cart shown in Figure 10 is built with an aluminium base and low friction passive wheels for stability. A central wheel which is not used for stabilisation is connected to a 500 ppr encoder for positioning monitoring. A motor is fixed centrally on the chassis and is driven through a 30:1 planetary gearbox. This has a 500 ppr encoder which is connected directly to the gearbox shaft of the motor and is used for angle monitoring.

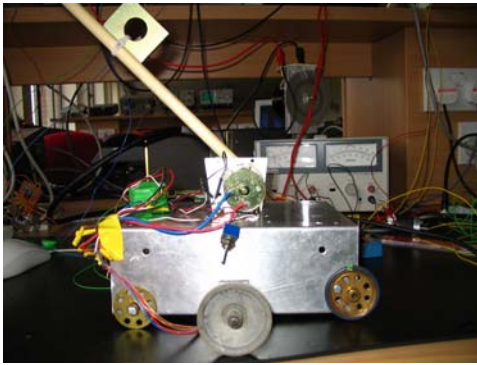
All electrical connections are routed via an umbilical cord with narrow gauge wire so as not to impede lateral motion. The total mass of the cart with motors and encoders is 923g. The motor drives a pendulum of length of 0.165m. A mass of 119g is connected to the end of the pendulum and the initial angle of the pendulum is fixed using a stop at 134 degrees. The static and dynamic friction coefficients were found to be $\mu = 0.014$ and $\mu = 0.0059$, respectively.

The minimum torque required to lift the pendulum from 0° is calculated from

$$\tau = F \times l \quad (3)$$

where τ is the torque delivered by the motor, F is the force exerted by the mass due to gravity, and l is the pendulum length. This minimum torque is therefore 0.193 Nm. The chosen sample rate is therefore 10 ms and, with the calculated low angular velocity of the pendulum, this represents a resolution of movement of less than 1° .

Figure 10 Experimental rig of the pendulum-driven cart-pole system (see online version for colours)



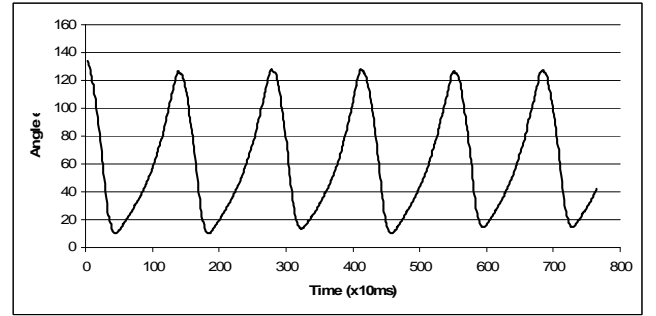
4.1 Experiment results

The proposed switch control law (2) is applied in a computer program to output the torques for the angles. The detailed control law used in the experiment is

$$\tau = \begin{cases} 0.35 & \theta(k) \in [180^\circ, 110^\circ) \\ 0.2 & \theta(k) \in [110^\circ, 40^\circ), \theta(k+1) - \theta(k) < 0 \\ -0.2 & \theta(k) \in [40^\circ, 0^\circ), \theta(k+1) - \theta(k) < 0 \\ -0.2 & \theta(k) \in [0^\circ, 90^\circ), \theta(k+1) - \theta(k) \geq 0 \\ -0.1 & \theta(k) \in [90^\circ, 120^\circ], \theta(k+1) - \theta(k) \geq 0 \end{cases} \quad (4)$$

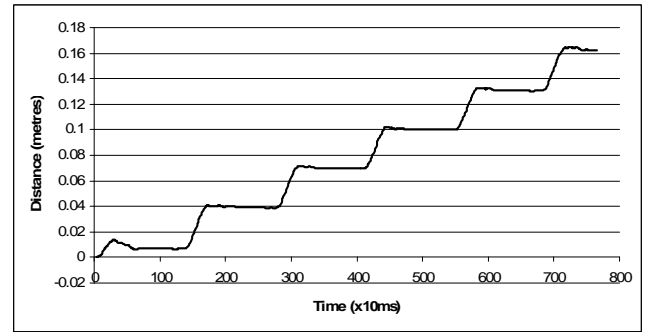
This resulted in a smooth operation of the pendulum oscillating between 125° and 18° shown in Figure 11.

Figure 11 The pendulum angle from an angle indexed torque profile



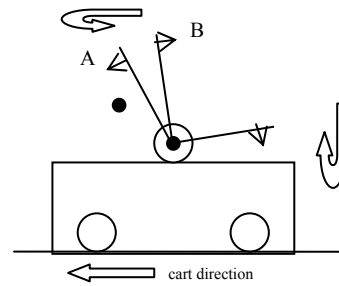
The cart made steady progress and reached 16 cm in 7.5 seconds, as shown in Figure 12. The average speed is about 2.13 cm/s.

Figure 12 The cart position from a time indexed torque profile



4.2 Detail of a single stroke cycle

Figure 13 Pendulum directions and positions



A single stroke cycle shown in Figure 14 was investigated and the speed obtained by taking the average of the difference of the current and previous two cart positions.

From Figure 14, point A shows the pendulum on its return stroke nearing its starting position; the change of direction occurs when the pendulum is almost vertical resulting in a force to the normal of this in the horizontal direction. Point C shows the pendulum reversing its stroke when almost horizontal resulting in a normal force on the vertical plane: the constraints of the surface prohibit its movement.

Figure 14 shows the results when the cart has been stationary for the return stroke and is coming to the end of its stationary period.

Figure 14 Single pendulum stroke

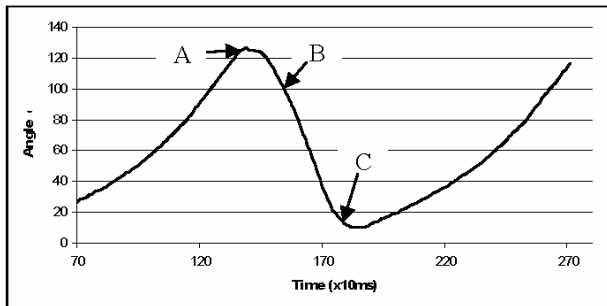
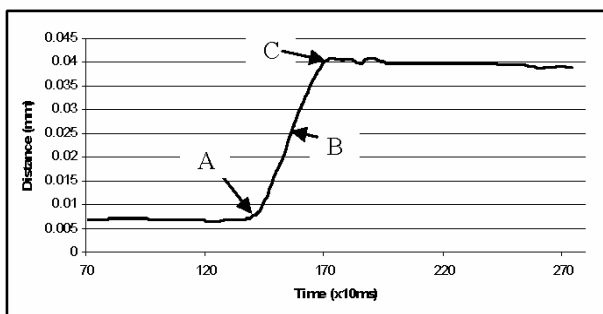
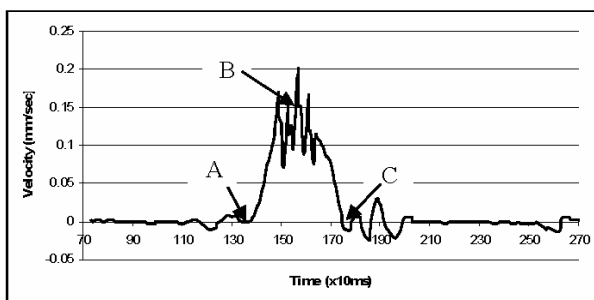


Figure 15 Cart movements during this single stroke



The pendulum reverses its direction as shown in point B of Figure 14. It is at this point of the pendulum reversing and accelerating in the opposite direction that the greatest velocity occurs (Figure 16) and the cart covers the greatest distance (Figure 15). The cart progresses until the pendulum is at its end of travel (point C) and the cart remains stationary until the next reversing pendulum stroke.

Figure 16 Cart velocities during single stroke

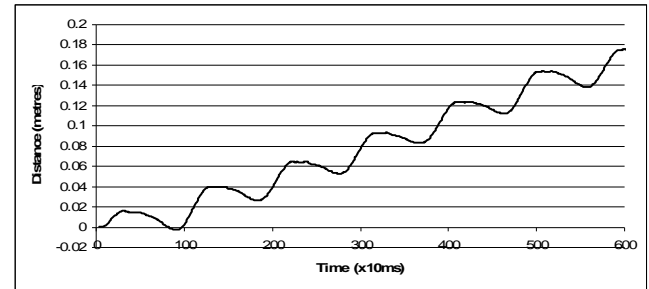


A different control law (5) was experimented with by changing the torque values and the angle boundaries so that each one is activated.

$$\tau = \begin{cases} 0.35 & \theta(k) \in [180^\circ, 110^\circ) \\ 0.2 & \theta(k) \in [110^\circ, 40^\circ), \theta(k+1) - \theta(k) < 0 \\ -0.3 & \theta(k) \in [40^\circ, 0^\circ), \theta(k+1) - \theta(k) < 0 \\ -0.3 & \theta(k) \in [0^\circ, 70^\circ), \theta(k+1) - \theta(k) \geq 0 \\ -0.2 & \theta(k) \in [70^\circ, 90^\circ), \theta(k+1) - \theta(k) \geq 0 \\ -0.1 & \theta(k) \in [90^\circ, 120^\circ), \theta(k+1) - \theta(k) \geq 0 \end{cases} \quad (5)$$

The results showed the cart made greater progress (taking six seconds to reach the previous distance of 18 cm) but also slipped back to a large degree on the return stroke (Figure 17) due to the increased acceleration of the return stroke. This shows that the motion of the cart is controllable by altering the torque profile using angle as an index. It also shows that optimisation of the torque profile could result in a more efficient progress.

Figure 17 Updated cart progress



5 Conclusions

For the ‘pendulum-driven cart’ problem, in contrast to the mathematical-oriented approaches used before, a new method based on some key concepts in advanced non-linear control and some physical insights is presented in this paper. The switch controller is simple and robust, yet achieves better performance in both simulation studies and experimental works. A further exploration of the significance of the research on this system is also presented.

Acknowledgements

The authors would like to thank the EPSRC research council (research grant EP/E025 250/1) for the support of this research and Dr. Emma Price for the technical support in producing this paper.

References

- Chernousko, F.L. (2001) ‘Controllable motions of a two-link mechanism along a horizontal plane’, *Journal of Applied Mathematics and Mechanics*, Vol. 65, pp.578–91.
- Chernousko, F.L. (2002) ‘The optimum rectilinear motion of a two-mass system’, *Journal of Applied Mathematics and Mechanics*, Vol. 66, pp.1–7.
- Li, H., Furuta, K. and Chernousko, F.L. (2005) ‘A pendulum-driven cart via internal force and static friction’, *Proceedings of the Conference on Physics and Control*, St. Petersburg, Russia.
- Liu, Y., Yu, H. and Burrows, B. (2007) ‘Optimization and control of a pendulum-driven cart-pole system’, *Proceedings of the 2007 IEEE International Conference on Networking, Sensing and Control*, London, UK, April.
- Wane, S.O., Yu, H. and Yang, T.C. (2007) ‘Development of a reaction drive for a propulsion mechanism’, *Proceedings of the 2007 IEEE International Conference on Networking, Sensing and Control*, London, UK, April.

- Yu, H., Liu, Y. and Yang, T.C. (2008) 'Closed-loop tracking control of a pendulum-driven cart-pole underactuated system', *Proceedings of the Institution of Mechanical Engineers, Part I, Journal of Systems and Control Engineering*, Vol. 222, No. 12, pp.109–125.